2013 European Control Conference (ECC)
July 17-19, 2013, Zürich, Switzerland.

LPV Observer Design and Damping Control of Container Crane Load Swing

A. M. Gonzalez, C. Hoffmann, C. Radisch and H. Werner, *Member, IEEE*

Abstract— **This paper presents advances in the damping of container crane load swing via hoisting modulation based on linear parameter-varying (LPV) control techniques. We propose controllers based on constant, as well as parameter-dependent Lyapunov functions and formulate our problem in the linear fractional transformation (LFT) framework. The dynamics of a nonlinear observer are included into the generalized plant. Simulation and experimental results are compared to previous work using a polytopic LPV approach, as well as to earlier work based on the concept of resonant coupling control realized by a reduced normal form approach. The comparison indicates, that including the observer dynamics in the synthesis comes at the price of reduced performance, which is alleviated by the use of parameter-dependent Lyapunov functions. Furthermore, an a posteriori analysis verifies that the controller is robust against erroneously estimated scheduling signals and thus provides closed-loop guarantees for stability and performance for the new controller.**

I. Introduction

Reducing load swing during the loading and unloading processes of container cargo leads to increased efficiency and thus reduced costs. This has gained attention due to an increasing amount of cargo transported by freight ships. We propose a controller and observer design for the problem of damping load swing by modulation of the hoisting velocity. Here, the major difficulty resides in the fact that the mathematical coupling between the angular oscillation and the dynamics in direction of the rope is lost when the model is linearized, making nonlinear control approaches mandatory [1]. The system is underactuated and the damping of oscillations via hoisting modulation and tracking a reference in the rope length are conflicting control objectives. Our previous approach consists in the design of a polytopic linear parameter-varying (LPV) controller [1] , which relies on an observer in the form of an unscented Kalman filter [2], that has been used in conjunction with a so-called normal form controller. We refer the interested reader to [1] for a more thorough review of previous approaches.

The LPV framework is attractive as it is often feasible for the control of nonlinear plants in a quasi-LPV representation, which means that scheduling signals may consist of states, inputs and outputs, rather than exogeneous signals [3], [4], [5], [6]. In general, the synthesis approaches guarantee closed-loop stability and performance in the entire parameter range as long as measurements of the scheduling signals are available. In our previous approach, the observer dynamics and possible estimation errors have not been taken into account. As some of the scheduling signals depend on the observed states, the guarantees have been rendered void. Furthermore, synthesis has been carried out based on a constant Lyapunov function (CLF), which is known to be conservative in general.

Contributions: In this paper, we present an LPV controller design using the linear fractional transformation (LFT) framework, which takes into account the dynamics of a nonlinear observer (similarly to what was successfully done in [7]), while we also investigate the performance increase obtained by employing parameter-dependent Lyapunov functions (PDLF). In contrast to existing synthesis approaches for polytopic LPV systems that directly take into account inexact scheduling parameters [8], [9] via a bilinear matrix inequality (BMI) problem formulation, we have chosen to further propose an a posteriori analysis, which is used to verify that the closed-loop is robust against deviations within known bounds in the scheduling signals.

Outline of the Paper: Section II briefly reviews LFT-LPV model representations. Section III deals with plant modelling, observer design and the augmented plant model, including the observer. Controller design is covered in Section IV, where also robustness against inexact scheduling signals is analysed. Experimental and simulation results are presented and conclusions are drawn in Sections V and VI, respectively.

Notation: An (upper) linear fractional transformation is denoted by $\Delta \star M$, with definition $M_{22} + M_{21}\Delta(I - M_{11}\Delta)^{-1}M_{12} = \Delta \star \left[\begin{array}{c:c} M_{11} & M_{12} \\ \hdashline M_{21} & M_{22} \end{array}\right]$. Time dependence of scheduling parameters is regularly dropped, e.g. $\theta = \theta(t)$.

II. LFT-LPV Models and Closed-Loop Analysis

Consider an LFT parameter-dependent plant of the form

$$\mathcal{P}: \begin{cases} \begin{bmatrix} \dot{x}^P \\ \hdashline z_\Theta^P \\ z_\mathrm{p} \\ y \end{bmatrix} = \left[\begin{array}{c:ccc} A & B_\Theta & B_\mathrm{p} & B_u \\ \hdashline C_\Theta & D_{\Theta\Theta} & D_{\Theta\mathrm{p}} & D_{\Theta u} \\ C_\mathrm{p} & D_{\mathrm{p}\Theta} & D_{\mathrm{pp}} & D_{\mathrm{p}u} \\ C_y & D_{y\Theta} & D_{y\mathrm{p}} & D_{yu} \end{array}\right] \begin{bmatrix} x^P \\ \hdashline w_\Theta^P \\ w_\mathrm{p} \\ u \end{bmatrix}, \\ \quad w_\Theta^P = \Theta^P z_\Theta^P, \end{cases} \tag{1}$$

where $x^P \in \mathbb{R}^{n_x^P}$, $u \in \mathbb{R}^{n_u}$, $y \in \mathbb{R}^{n_y}$, $w_\mathrm{p} \in \mathbb{R}^{n_\mathrm{p}}$, $z_\mathrm{p} \in \mathbb{R}^{n_\mathrm{p}}$, $w_\Theta^P \in \mathbb{R}^{n_\Theta^P}$, $z_\Theta^P \in \mathbb{R}^{n_\Theta^P}$ are the state, input, output, performance and scheduling signal vectors of the system, respectively. Assume, that the LFT representation is well-posed,

A. M. Gonzalez, C. Hoffmann and H. Werner are with the Institute of Control Systems, Hamburg University of Technology, Eißendorfer Str. 40, 21073 Hamburg, Germany e-mail: {antonio.mendez, christian.hoffmann, h.werner}@tu-harburg.de.

C. Radisch is with the Institute of Mechanics and Ocean Engineering, Hamburg University of Technology, Eißendorfer Str. 42, 21073 Hamburg, Germany e-mail: christian.radisch@tu-harburg.de.

i.e. $(I - D_{\Theta\Theta}\Theta^P)$ is invertible for all admissible parameter values. For an LFT-LPV plant we assume $\Theta^P(t)$ to have block-diagonal structure, i.e. $\Theta^P(t) = \bigoplus_{i\in\boldsymbol{i}_\Theta} \theta_i I_{r_i^P}$, where $\sum_{i\in\boldsymbol{i}_\Theta} r_i^P = n_\Theta^P$. The vector $\theta(t) = [\theta_1(t)\ \theta_2(t)\ \dots\ \theta_{n_\theta}(t)]$ collects all scheduling parameters, whose values are bounded. With $\boldsymbol{i}_\Theta = \{1, \dots, n_\theta\}$, typically we define $\theta \in \boldsymbol{\theta} = \{\theta \mid |\theta_i| \leqslant 1,\ i \in \boldsymbol{i}_\Theta\}$. The time derivatives are also bounded, such that $\dot\theta(t) = \nu(t) = [\nu_1(t)\ \dots\ \nu_{n_\theta}(t)]$, with $\nu \in \boldsymbol{\nu} = \{\nu \mid |\nu_i| \leqslant \bar\nu_i,\ i \in \boldsymbol{i}_\Theta\}$. Parameter-dependent state space matrices of the generalized plant are related to the LFT representation by

$$\begin{bmatrix} \mathscr{A}(\theta) & \mathscr{B}_\mathrm{p}(\theta) & \mathscr{B}_u(\theta) \\ \mathscr{C}_\mathrm{p}(\theta) & \mathscr{D}_\mathrm{pp}(\theta) & \mathscr{D}_{\mathrm{p}u}(\theta) \\ \mathscr{C}_y(\theta) & \mathscr{D}_{y\mathrm{p}}(\theta) & \mathscr{D}_{yu}(\theta) \end{bmatrix} = \begin{bmatrix} A & B_\mathrm{p} & B_u \\ C_\mathrm{p} & D_\mathrm{pp} & D_{\mathrm{p}u} \\ C_y & D_{y\mathrm{p}} & D_{yu} \end{bmatrix} + \dots$$

$$\begin{bmatrix} B_\Theta \\ D_{\mathrm{p}\Theta} \\ D_{y\Theta} \end{bmatrix} \Theta^P (I - D_{\Theta\Theta}\Theta^P)^{-1} [C_\Theta\ D_{\Theta\mathrm{p}}\ D_{\Theta u}].$$

An LFT-LPV controller is given by

$$\mathcal{K} : \begin{cases} \begin{bmatrix} \dot x^K \\ \hline u \\ z_\Theta^K \end{bmatrix} = \begin{bmatrix} A^K & B_y^K & B_\Theta^K \\ \hline C_u^K & D_{uy}^K & D_{u\Theta}^K \\ C_\Theta^K & D_{\Theta y}^K & D_{\Theta\Theta}^K \end{bmatrix} \begin{bmatrix} x^K \\ \hline y \\ w_\Theta^K \end{bmatrix}, \\ w_\Theta^K = \mathrm{diag}\left(\Theta^K, \dot\Theta^K\right) z_\Theta^K = \tilde\Theta^K z_\Theta^K, \end{cases} \tag{2}$$

where $x^K \in \mathbb{R}^{n_x^K}$, $w_\Theta^K \in \mathbb{R}^{n_\Theta^K}$, $z_\Theta^K \in \mathbb{R}^{n_\Theta^K}$ and $\Theta^K = \bigoplus_{i\in\boldsymbol{i}_\Theta} \theta_i I_{r_i^K}$. The parameter-dependent state space matrices of the controller are computed by

$$\begin{bmatrix} \mathscr{A}^K(\theta, \dot\theta) & \mathscr{B}^K(\theta) \\ \mathscr{C}^K(\theta) & \mathscr{D}^K(\theta) \end{bmatrix} = \begin{bmatrix} A^K & B_y^K \\ C_u^K & D_{uy}^K \end{bmatrix} + \dots$$

$$\begin{bmatrix} B_\Theta^K \\ D_{u\Theta}^K \end{bmatrix} \tilde\Theta^K (I - D_{\Theta\Theta}^K \tilde\Theta^K)^{-1} \left[C_\Theta^K\ D_{\Theta y}^K\right].$$

From the notation used in (1), the symbol $\mathcal{P}$ denotes the input-output map obtained when $\mathcal{P} = \mathrm{diag}\left(\frac{1}{s}I, \Theta^P\right) \star P$, where P denotes the matrix defined in (1).

With the above definitions, we may introduce the following augmented closed-loop matrices

$$\mathcal{H}(\theta) = \Theta \star \begin{bmatrix} \mathcal{H}_{11} & \mathcal{H}_{12} \\ \mathcal{H}_{21} & \mathcal{H}_{22} \end{bmatrix},\ \Theta = \mathrm{diag}\left(\Theta^P, \tilde\Theta^K\right), \tag{3}$$

$$\begin{bmatrix} \mathcal{H}_{11} & \mathcal{H}_{12} \\ \mathcal{H}_{21} & \mathcal{H}_{22} \end{bmatrix} = \left[\begin{array}{cc|cc} \mathcal{D}_{\Theta\Theta}^{PP} & \mathcal{D}_{\Theta\Theta}^{PK} & \mathcal{C}_\Theta^P & \mathcal{D}_{\Theta\mathrm{p}}^P \\ \mathcal{D}_{\Theta\Theta}^{KP} & \mathcal{D}_{\Theta\Theta}^{KK} & \mathcal{C}_\Theta^K & \mathcal{D}_{\Theta\mathrm{p}}^K \\ \hline 0 & 0 & I & 0 \\ \mathcal{B}_\Theta^P & \mathcal{B}_\Theta^K & \mathcal{A} & \mathcal{B}_\mathrm{p} \\ 0 & 0 & 0 & I \\ \mathcal{D}_{\mathrm{p}\Theta}^P & \mathcal{D}_{\mathrm{p}\Theta}^K & \mathcal{C}_\mathrm{p} & \mathcal{D}_\mathrm{pp} \end{array}\right] = \left[\begin{array}{cc|cc|c} D_{\Theta\Theta} & 0 & C_\Theta & 0 & D_{\Theta\mathrm{p}} \\ 0 & 0 & 0 & 0 & 0 \\ \hline 0 & 0 & I & 0 & 0 \\ 0 & 0 & 0 & I & 0 \\ \hline B_\Theta & 0 & A & 0 & B_\mathrm{p} \\ 0 & 0 & 0 & 0 & 0 \\ \hline 0 & 0 & 0 & 0 & I \\ \hline D_{\mathrm{p}\Theta} & 0 & C_\mathrm{p} & 0 & D_\mathrm{pp} \end{array}\right] + $$

$$\dots \left[\begin{array}{ccc} 0 & 0 & D_{\Theta u} \\ I & 0 & 0 \\ \hline 0 & 0 & 0 \\ 0 & 0 & 0 \\ \hline 0 & 0 & B_u \\ 0 & I & 0 \\ \hline 0 & 0 & 0 \\ \hline 0 & 0 & D_{\mathrm{p}u} \end{array}\right] \left[\begin{array}{c|cc} D_{\Theta\Theta}^K & C_\Theta^K & D_{\Theta y}^K \\ \hline B_\Theta^K & A^K & B_y^K \\ D_{u\Theta}^K & C_u^K & D_{uy}^K \end{array}\right] \left[\begin{array}{cc|cc|c} 0 & I & 0 & 0 & 0 \\ 0 & 0 & 0 & I & 0 \\ D_{y\Theta} & 0 & C_y & 0 & D_{y\mathrm{p}} \end{array}\right] \tag{4}$$

We now present a condition using parameter-dependent Lyapunov functions in quadratic LFT form $\mathcal{X}(\theta) = T_\mathcal{X}^\top(\theta) Y T_\mathcal{X}(\theta)$ [6] for the analysis of closed-loop stability and performance. The theorem can be used to check whether controllers still yield the aforementioned guarantees, when they are synthesized based on approximate models [10], or — as in this paper — their scheduling policy is altered after synthesis (Section IV-B).

Theorem 1: The closed-loop system $\mathcal{P} \star \mathcal{K}$ is stable and has $\mathcal{L}_2$ gain less than $\gamma > 0$, $\forall\theta \in \boldsymbol{\theta}$ and $\forall\nu \in \boldsymbol{\nu}$, if there exist a quadratic LFT function $\mathcal{X}(\theta) = T_\mathcal{X}^\top(\theta) Y T_\mathcal{X}(\theta) > 0$ and a multiplier $\Pi = \Pi^\top$ that satisfy

$$\begin{bmatrix} \star \\ \hline \star \end{bmatrix}^\top \left[\begin{array}{c|cccc} \Pi & 0 & 0 & 0 & 0 \\ \hline 0 & 0 & Y & 0 & 0 \\ 0 & Y & 0 & 0 & 0 \\ 0 & 0 & 0 & -\gamma^2 I & 0 \\ 0 & 0 & 0 & 0 & I \end{array}\right] \left[\begin{array}{cc} \mathscr{B}_{11} & \mathscr{B}_{12} \\ I & 0 \\ \hline \mathscr{B}_{21} & \mathscr{B}_{22} \end{array}\right] < 0, \tag{5}$$

$$[\star]^\top \underbrace{\begin{bmatrix} \Pi_R & \Pi_S \\ \Pi_S^\top & \Pi_Q \end{bmatrix}}_{\Pi} \left[\begin{array}{cc} I & 0 \\ 0 & I \\ \hline \Delta_\mathcal{X} & 0 \\ 0 & \Theta \end{array}\right] > 0, \quad \forall(\theta, \nu) \in \boldsymbol{\theta} \times \boldsymbol{\nu}, \tag{6}$$

where $\Delta_\mathcal{X} = \mathrm{diag}\left(\dot\Theta_\mathcal{X}, \Theta_\mathcal{X}, \Theta_\mathcal{X}\right)$,

$$\left[\begin{array}{c|c} \mathscr{B}_{11} & \mathscr{B}_{12} \\ \hline \mathscr{B}_{21} & \mathscr{B}_{22} \end{array}\right] = \left[\begin{array}{cc|c} \mathscr{T}_{\mathcal{X}11} & \mathscr{T}_{\mathcal{X}12}\mathcal{H}_{21} & \mathscr{T}_{\mathcal{X}12}\mathcal{H}_{22} \\ 0 & \mathcal{H}_{11} & \mathcal{H}_{12} \\ \hline \mathscr{T}_{\mathcal{X}21} & \mathscr{T}_{\mathcal{X}22}\mathcal{H}_{21} & \mathscr{T}_{\mathcal{X}22}\mathcal{H}_{22} \end{array}\right],$$

$$\left[\begin{array}{c|c} \mathscr{T}_{\mathcal{X}11} & \mathscr{T}_{\mathcal{X}12} \\ \hline \mathscr{T}_{\mathcal{X}21} & \mathscr{T}_{\mathcal{X}22} \end{array}\right] = \left[\begin{array}{ccc|cccc} 0 & 0 & T_{\mathcal{X}11} & T_{\mathcal{X}12} & 0 & 0 & 0 \\ T_{\mathcal{X}11} & T_{\mathcal{X}11} & 0 & 0 & -T_{\mathcal{X}12} & 0 & 0 \\ 0 & 0 & T_{\mathcal{X}11} & T_{\mathcal{X}12} & 0 & 0 & 0 \\ \hline 0 & 0 & T_{\mathcal{X}21} & T_{\mathcal{X}22} & 0 & 0 & 0 \\ -T_{\mathcal{X}21} & -T_{\mathcal{X}21} & 0 & 0 & T_{\mathcal{X}22} & 0 & 0 \\ 0 & 0 & 0 & 0 & 0 & I & 0 \\ 0 & 0 & 0 & 0 & 0 & 0 & I \end{array}\right],$$

$$T_\mathcal{X}(\theta) = \Theta_\mathcal{X} \star \left[\begin{array}{c|c} T_{\mathcal{X}11} & T_{\mathcal{X}12} \\ \hline T_{\mathcal{X}21} & T_{\mathcal{X}22} \end{array}\right].$$

Proof: The proof follows along the ideas presented in [6], where they are applied to the projected version of the parameter-dependent Bounded Real Lemma [11]. ■

III. LPV Modelling and Observer Design

A. Plant Description

At the test bench available at the *Institute of Mechanics and Ocean Engineering*, *Hamburg University of Technology*, a container is held by four ropes and hoisted by winches along the $\mathbf{z}$ axis. Moreover, a trolley can move the container along the $\mathbf{x}$ axis. In Fig. 1 a simplified version of the crane is depicted. The reader can refer to [12] to find a complete description of the physical setup and components of the test bench. The physical dimensions of the states are $L \in [3, 12]$ m, $\dot L \in [-2, 2]$ m s^{-1}, $\phi \in [-0.2,\ 0.2]$ rad and $\dot\phi \in [-0.25,\ 0.25]$ rad s^{-1}.

The control objectives of the container crane problem can be stated as follows: *(i)* Damp angular oscillations in the eigen-frequency range and *(ii)* Track rope length and hoisting velocity reference commands L_ref and $\dot L_\mathrm{ref}$. As can be seen in Fig. 2, L_ref is computed from $\dot L_\mathrm{ref}$, in the sense that it represents a ramp when $\dot L_\mathrm{ref} \neq 0$ (hoisting) and it is constant when $\dot L_\mathrm{ref} = 0$ (damping). Due to the nature of the nonlinear coupling, the need for an oscillatory motion in L arises (with $\dot L = 0$ there is no coupling), leading to conflicting

(a) Schematic crane representation (b) Photo of the test bench

Fig. 1. Schematic crane representation and photo of the actual test bench

objectives, e.g. damping ϕ would cause the controlled system to deviate L and $\dot{L}$ from its reference commands. This A simple model is given when no trolley movement and only planar motion of the container are considered, therefore the nonlinear equations are those of a damped pendulum with variable length L and angular displacement ϕ [1].

$$\ddot{\phi} = -g\frac{\sin\phi}{L} - d\dot{\phi} - 2\frac{\dot{\phi}\dot{L}}{L} \tag{7}$$

An internal control loop performs synchronous hoisting velocity tracking control at the rope winches' drive level. A simple description of the resulting dynamics is given by the first order model with time constant $\tau = 0.1$ s.

$$\ddot{L} = -\frac{1}{\tau}\dot{L} + \frac{1}{\tau}u. \tag{8}$$

A suitable nonlinear state space representation is motivated in [1] and given below. Notice the nonlinear coupling between modes ϕ and L in the term $-2\frac{\dot{\phi}}{L}$:

$$\mathcal{M}: \left\{ \begin{bmatrix} \dot{\phi} \\ \ddot{\phi} \\ \dot{L} \\ \ddot{L} \\ \hdashline y \end{bmatrix} = \begin{bmatrix} 0 & 1 & 0 & 0 \\ -\frac{g\sin\phi}{L\phi} & -d & 0 & -2\frac{\dot{\phi}}{L} \\ 0 & 0 & 0 & 1 \\ 0 & 0 & 0 & -\tau^{-1} \\ \hdashline & I & & \end{bmatrix} \begin{bmatrix} \phi \\ \dot{\phi} \\ L \\ \dot{L} \end{bmatrix} + \begin{bmatrix} 0 \\ 0 \\ 0 \\ \tau^{-1} \\ \hdashline 0 \end{bmatrix} u. \right. \tag{9}$$

At the test bench, the measured variables are L, $\dot{L}$ and the rope forces $F^{\top} = [F_1\ F_2\ F_3\ F_4]$, where $F_j,\ j \in \{1,2,3,4\}$ represents the force acting in each rope. The following formula computes ϕ based on the force measurements.

$$\phi(F) = \tan^{-1}\left(\frac{a}{c}\frac{F_1 - F_2 - F_3 + F_4}{F_1 + F_2 + F_3 + F_4}\right) \tag{10}$$

The above equation is derived via torque equilibria analysis [13], where a and c denote the coordinates of the center of gravity of the container on the **x**-**z** plane. Notice that using Eq. (10) will propagate noise from the force measurements to ϕ, and thus taking the time derivative to obtain $\dot{\phi}$ is impractical. Therefore an observer based approach is employed.

B. Observer Design

The motivation for replacing the existing unscented Kalman filter from [2] with an LPV observer lies in the fact, that its dynamics are more easily included in the generalized plant for the subsequent controller synthesis. The design methodology is taken from [14], which considers nonlinear systems with noisy measurements of the form:

$$\dot{x} = f(x, u), \quad y = h(x) + Dd_n. \tag{11}$$

For the above system, a nonlinear Luenberger observer (12) with constant gain V is optimized, via LMIs, in terms of noise reduction.

$$\dot{\hat{x}} = f(\hat{x}, u) + V\left(h(\hat{x}) - y\right), \tag{12}$$

Since L and $\dot{L}$ are measurable directly, the model of the crane used for the observer design does not regard these as states but as inputs:

$$\ddot{\phi} = -g\sin\phi u_1 - d\dot{\phi} - 2\dot{\phi}u_2,\ \ y = \phi, u_1 = \tfrac{1}{L}, u_2 = \tfrac{\dot{L}}{L}.$$

The proposed observer equations for the above system are:

$$\mathcal{O}: \left\{ \begin{array}{l} \begin{bmatrix} \dot{\hat{\phi}} \\ \ddot{\hat{\phi}} \end{bmatrix} = \begin{bmatrix} \dot{\hat{\phi}} \\ -g\sin\hat{\phi}u_1 - d\dot{\hat{\phi}} - 2\dot{\hat{\phi}}u_2 \end{bmatrix} + \begin{bmatrix} V_1 \\ V_2 \end{bmatrix}(\hat{\phi} - \phi(F)), \\ \hat{y} = [\hat{\phi}\ \dot{\hat{\phi}}]^{\top}. \end{array} \right.$$

where the observer gain is found by solving the optimization problem proposed in [14], which is then given by $V^{\top} = \begin{bmatrix} V_1 & V_2 \end{bmatrix} = \begin{bmatrix} -2.169 & -1.061 \end{bmatrix}$.

C. LPV-LFT Model

Once the observer has been designed it can be included into the crane model (9), which yields the state equation

$$\begin{bmatrix} \dot{\phi} \\ \ddot{\phi} \\ \dot{L} \\ \ddot{L} \\ \hdashline \dot{\hat{\phi}} \\ \ddot{\hat{\phi}} \end{bmatrix} = \begin{bmatrix} 0 & 1 & 0 & 0 & \vdots & 0 & 0 \\ -\frac{g\sin\phi}{L\phi} & -d & 0 & -2\frac{\dot{\phi}}{L} & \vdots & 0 & 0 \\ 0 & 0 & 0 & 1 & \vdots & 0 & 0 \\ 0 & 0 & 0 & -\tau^{-1} & \vdots & 0 & 0 \\ \hdashline -V_1 & 0 & 0 & 0 & \vdots & V_1 & 1 \\ -V_2 & -d & 0 & -2\frac{\dot{\hat{\phi}}}{L} & \vdots & V_2 - \frac{g\sin\hat{\phi}}{L\hat{\phi}} & 0 \end{bmatrix} \begin{bmatrix} \phi \\ \dot{\phi} \\ L \\ \dot{L} \\ \hdashline \hat{\phi} \\ \dot{\hat{\phi}} \end{bmatrix} + \begin{bmatrix} 0 \\ 0 \\ 0 \\ \tau^{-1} \\ \hdashline 0 \\ 0 \end{bmatrix} u.$$

Notice that the above system contains several nonlinearities. The following remedies are proposed:

- Since $\frac{\sin\alpha}{\alpha} \approx 1$ for small angles α relevant in the control problem, two parameters can be avoided.
- Taking into account $\dot{\phi}$ and $\dot{\hat{\phi}}$ as two distinct scheduling parameters is conservative. We propose a coupling $\dot{\hat{\phi}} = \dot{\phi} + \delta_{\dot{\phi}}$ with a known bound $|\delta_{\dot{\phi}}| \leqslant 0.02$ rad s^{-1} on the deviation. The proposed range for $\delta_{\dot{\phi}}$ should match the actual deviation which can be determined experimentally by validating the observer accuracy with a camera system.

The above leads to a simplified nonlinear state space representation

$$\tilde{\mathcal{G}}: \left\{ \begin{bmatrix} \dot{\phi} \\ \ddot{\phi} \\ \dot{L} \\ \ddot{L} \\ \hdashline \dot{\hat{\phi}} \\ \ddot{\hat{\phi}} \\ \hdashline \tilde{y} \end{bmatrix} = \begin{bmatrix} 0 & 1 & 0 & 0 & \vdots & 0 & 0 \\ -\frac{g}{L} & -d & 0 & -2\frac{\dot{\hat{\phi}} - \delta_{\dot{\phi}}}{L} & \vdots & 0 & 0 \\ 0 & 0 & 0 & 1 & \vdots & 0 & 0 \\ 0 & 0 & 0 & -\tau^{-1} & \vdots & 0 & 0 \\ \hdashline -V_1 & 0 & 0 & 0 & \vdots & V_1 & 1 \\ -V_2 & -d & 0 & -2\frac{\dot{\hat{\phi}}}{L} & \vdots & V_2 - \frac{g}{L} & 0 \\ \hdashline & & & I & & & \end{bmatrix} \begin{bmatrix} \phi \\ \dot{\phi} \\ L \\ \dot{L} \\ \hdashline \hat{\phi} \\ \dot{\hat{\phi}} \end{bmatrix} + \begin{bmatrix} 0 \\ 0 \\ 0 \\ \tau^{-1} \\ \hdashline 0 \\ 0 \\ \hdashline 0 \end{bmatrix} u. \right. \tag{13}$$

For the above representation a parameter vector $\theta^\top = [\theta_1\ \theta_2\ \theta_3] = [\hat{\dot{\phi}}\ \frac{1}{L}\ \delta_{\dot{\phi}}]$ is defined. Using MATLAB's *Robust Control Toolbox*, an LFT representation with parameter block $\Theta^P = \mathrm{diag}(\theta_1,\, \theta_2 I_2,\, \theta_3)$. System (9) with the above simplifications is denoted as $\tilde{\mathcal{M}}$. Notice that the LPV system (13) is actually a quasi-LPV system.

IV. Controller Design

The synthesis algorithm used in this work can be found in [6]. The method is based on the parameter-dependent Bounded Real Lemma with parameter-dependent Lyapunov functions (e.g. [15]), where an infinite dimensional set of LMIs has to be satisfied to prove the existence of a controller that stabilizes the closed-loop system and minimizes its induced $\mathcal{L}_2$ norm. The full-block $\mathcal{S}$-Procedure [5] is applied to render the problem finite dimensional. However, to be able to do that, it is required to express the Lyapunov matrices in a quadratic LFT form $R(\theta) = T_R^T(\theta) X T_R(\theta)$ and $S(\theta) = T_S^T(\theta) Y T_S(\theta)$. The optimization is performed over coefficient matrices X and Y that determine the Lyapunov matrices from a search space defined by the design parameters $T_R(\theta)$ and $T_S(\theta)$, which need to be provided as LFT functions of θ.

A. Generalized Plant

A mixed sensitivity shaping approach will be utilized to enforce the desired closed-loop behaviour. The generalized plant, represented by $\tilde{\mathcal{P}}$, is depicted in Fig. 2. Which includes

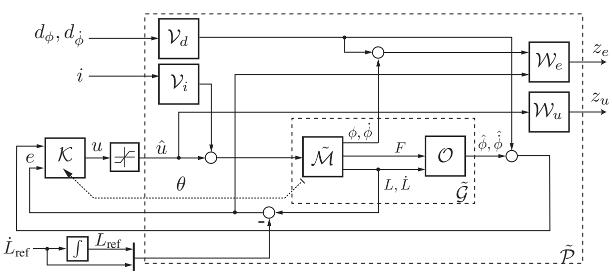

Fig. 2. Control Loop for the Container Crane

the augmented crane model $\tilde{\mathcal{G}}$ and the shaping filters $\mathcal{V}_i$, $\mathcal{V}_d$, $\mathcal{W}_e$ and $\mathcal{W}_u$. Those filters are intended to shape the sensitivity functions $\mathcal{S}$, $\mathcal{S}\tilde{\mathcal{G}}$, $\mathcal{KS}$ and $\mathcal{KS}\tilde{\mathcal{G}}$, where $\mathcal{S} = (I - \tilde{\mathcal{G}}\mathcal{K})^{-1}$. Five exogenous signals are introduced: Two reference signals L_{ref}, $\dot{L}_{\text{ref}}$ for L and $\dot{L}$, two output disturbances d_ϕ, $d_{\dot{\phi}}$ for ϕ and $\dot{\phi}$ and an input disturbance i for u. The output disturbances reflect influence of wind or trolley movement, while the input disturbances occur due to friction between ropes and pulleys, elasticity of the ropes and the rope winch cascade control structure. Performance outputs z_e and z_u are used to specify the disturbance attenuation, reference tracking and control action objectives.

Note, that the performance objectives defined by the filter $\mathcal{W}_e$ are formulated with respect to the actual states ϕ, $\dot{\phi}$ of the crane, which are not measured, instead of the observed states, which are fed to the controller. Since only the observed state $\hat{\dot{\phi}}$ is available for scheduling the controller, the synthesis will not guarantee stability and performance, as a fundamental assumption in most current LPV control approaches — exact knowledge of the scheduling signals $\theta(t)$ — is violated. The scheduling parameter $\delta_{\dot{\phi}}$ will be unknown, as $\dot{\phi}$ is assumed to be known only up to a maximum deviation $\bar{\delta}_{\dot{\phi}}$ as $\delta_{\dot{\phi}} \leqslant \bar{\delta}_{\dot{\phi}} = |\hat{\dot{\phi}} - \dot{\phi}| = 0.02\ \mathrm{rad\,s^{-1}}$. Refer to Section IV-B for further discussion.

Let $\mathcal{T}_{zw}$ represent the mapping from $w = [d_\phi\ d_{\dot{\phi}}\ L_{\text{ref}}\ \dot{L}_{\text{ref}}\ i]^\top$ to $z = [z_e\ z_u]^\top$. The objective is to find a controller $\mathcal{K}$, such that the induced $\mathcal{L}_2$ norm of $\mathcal{T}_{zw}$ is minimized: $\gamma = \min_{\mathcal{K}} \|\mathcal{T}_{zw}\|_{\mathcal{L}_2}$. The input disturbance filter and sensitivity filter are multi-input filters and they have the following structure:

$$\mathcal{V}_d = \mathrm{diag}\Big(\mathcal{V}_\phi,\ \mathcal{V}_{\dot{\phi}}\Big), \qquad \mathcal{W}_e = \Big[\mathcal{W}_\phi \quad \mathcal{W}_{\dot{\phi}} \quad \mathcal{W}_L \quad \mathcal{W}_{\dot{L}}\Big]$$

Notice that $\mathcal{W}_e$ is not in the typical block diagonal form, since only one singular value in $\mathcal{S}$ can be shaped. The reason for that is due to the underactuated nature of the crane, i.e. only one input is provided while four outputs are to be controlled. As a consequence, the rank of $\mathcal{GK}$ is only 1 (for frozen parameters θ over all frequencies).

CLF and PDLF approaches have been used to synthesize a controller, with the following weighting filters:

$$\mathcal{W}_\phi = \mathcal{W}_{\dot{L}} = 0,\ \mathcal{W}_{\dot{\phi}} = \frac{4}{s+0.01},\ \mathcal{W}_L = \frac{2.3}{s+0.01},\ \mathcal{V}_i = 0.7,$$
$$\mathcal{W}_u = \frac{200(s+10)}{s+10^4},\ \mathcal{V}_\phi = 1,\ \mathcal{V}_{\dot{\phi}} = \frac{10^{-3}(s+0.05)(s+20)}{(s+1)^2}.$$

Above filters, mainly impose different weight on tracking L and damping ϕ. Disturbances in the bandwidth of resonance frequencies are also suppressed. Tuning has been performed as to limit the control signal to the physical constraints of the rope winches, i.e. $|u| \leq 2\ \mathrm{m\,s^{-1}}$ and to reduce the effect of input disturbances.

Constant Lyapunov Functions: In the case of CLF no further design considerations are required. The algorithm provided in [6] has been implemented in MATLAB and the semi-definite program solver SeDuMi [16] via the interface YALMIP [17] has been used. A performance index $\gamma = 9.49$ has been obtained.

Parameter Dependendet Lyapunov Functions: A PDLF approach is less conservative since it involves information of the parameter's rate of change bounds. Having both $R(\theta)$ and $S(\theta)$ parameter-dependent, may yield impractical controllers [18], i.e. controllers that require online information on the time derivatives of the scheduling parameters. A PDLF based controller synthesis yields practically feasible controllers, if e.g. one of the decision variables $R(\theta)$ and $S(\theta)$ is chosen to be non-parameter-dependent. In this case, the controller does not depend on the time derivatives of scheduling signals. To see this, refer to [6] for formulae with which the controller is constructed after having solved the corresponding synthesis LMIs. In the case of practically valid PDLF based controllers, the formulae simplify to the ones below, where parameter dependencies are omitted for brevity.

$$M = I - RS, \quad N^\top = I, \tag{14a}$$

$$\mathscr{A}^K = -\Big(\mathscr{A}^\top + S\big[\mathscr{A} + \mathscr{B}_u F + L\mathscr{C}_y\big]R + \dots$$
$$\dots + \gamma^{-1} S\big[\mathscr{B}_\mathrm{p} + L\mathscr{D}_\mathrm{yp}\big]\mathscr{B}_\mathrm{p}^\top + \dots$$
$$\dots + \gamma^{-1}\mathscr{C}_\mathrm{p}^\top\big[\mathscr{C}_\mathrm{p} + \mathscr{D}_\mathrm{pu}F\big]R\Big)M^{-\top}, \tag{14b}$$

$$\mathscr{B}^K = SL, \quad \mathscr{C}^K = FRM^{-\top}. \tag{14c}$$

Symbolic tools from MATLAB's *Robust Control Toolbox* can then easily be employed to derive an LFT representation (2) from $\mathscr{A}^K, \mathscr{B}^K, \mathscr{C}^K, \mathscr{D}^K$.

In summary, the decision lies in choosing either $R(\theta)$ or $S(\theta)$ to be parameter-dependent. For this problem it has been found that, choosing $R(\theta)$ parameter-dependent and $S(\theta) = S_0$, yields less conservative results. The following choice of a polynomial basis function has been made:

$$R(\theta) = T_R^\top(\theta) X T_R(\theta) = \begin{bmatrix} I & \dot{\hat{\phi}} I & \frac{1}{L} I \end{bmatrix} \begin{bmatrix} X_0 & X_1 & X_2 \\ X_1^T & X_3 & X_4 \\ X_2^T & X_4^T & X_5 \end{bmatrix} \begin{bmatrix} I \\ \dot{\hat{\phi}} I \\ \frac{1}{L} I \end{bmatrix},$$

$$= X_0 + \dot{\hat{\phi}}\tilde{X}_1 + \tfrac{1}{L}\tilde{X}_2 + \tfrac{\dot{\hat{\phi}}}{L}\tilde{X}_4 + \dot{\hat{\phi}}^2 X_3 + \left(\tfrac{1}{L}\right)^2 X_5 \tag{15}$$

where $\tilde{X}_k = X_k + X_k^\top, \ k \in \{1, 2, 4\}$. The following bounds on the rate of variation have been imposed:

$$\bar{\nu}_1 = 0.5 \quad \bar{\nu}_2 = 0.5 \quad \bar{\nu}_3 = \infty \quad \text{where} \quad \theta(t) = [\dot{\hat{\phi}} \ \tfrac{1}{L} \ \delta_{\dot{\phi}}]^\top.$$

Note, that the parameter ranges have been normalized to $|\theta_i| \leqslant 1, \ i \in \{1, 2, 3\}$ in the LFT representation. Therefore, the above values do not exhibit an immediate physical meaning as they represent the rates of variation of the normalized values. By making $R(\theta)$ independent from $\delta_{\dot{\phi}}$, we are allowing $\delta_{\dot{\phi}}$ to change infinitely fast.

When applying the full-block $\mathcal{S}$-procedure as in [6], constraints can be imposed on the structure of the multipliers, providing means to trade off conservatism versus computational complexity during synthesis. It has been observed, that skew-symmetric multipliers (also known as D-G-scalings) are too conservative for our purposes, in the sense that performance of the PDLF case, using D-G-scalings, is nearly the same as in the CLF case. Accordingly, full-block scalings with multiplier constraints in the vertices of the convex polytope spanned by the parameter ranges and bounds on the rates of change have been used and a performance index of $\gamma = 4.12$ has been obtained.

B. Robustness against Inexact Scheduling

As is obvious from Eq. 14, the controller is constructed from both plant and Lyapunov function data. To match the actual experimental setup, we substitute $\delta_{\dot{\phi}} = 0$ in the controller's scheduling policy. It is clear that if $\delta_{\dot{\phi}}$ is unknown, then the plant reconstruction will lose accuracy. However, for the PDLF the problem is avoided by excluding δ_ϕ from the definition of $R(\theta)$, i.e, the PDLF will depend only on certain parameters, as in Eq. (15). Notice that this also reduces the size of the multipliers required by the synthesis algorithm [6], which is beneficial for computational complexity. One can also do the same by forcing some blocks of X and Y to be 0, however this retains the size of the multipliers. By setting $\delta_{\dot{\phi}} = 0$ in the controller scheduling block, stability and performance guarantees are lost. However, these guarantees are recovered by solving the optimization problem associated with Theorem 1. As the a posteriori analysis can lead to numerical problems in the solver, the performance indices γ, from the synthesis, have been increased by 10% and used to solve feasibility problems instead. The analysis results have shown, that the closed-loop will remain stable and maintain performance guarantees.

V. Simulations and Experimental Results

The following two experiments assess the controller performance with respect to damping oscillations and tracking the reference length in simulations and on the test bench:

(i) Damping scenario: $\dot{L}_\mathrm{ref} = 0 \ \mathrm{m\,s^{-1}}$, $L_\mathrm{ref} = 6$ m.

(ii) Hoisting scenario: $\dot{L}_\mathrm{ref} = -0.2 \ \mathrm{m\,s^{-1}}$, $L_0 = 7.5$ m.

The controllers are discretized via bilinear approximation with a sampling time $T_\mathrm{s} = 0.01$ s.

Validation of Simulations: Comparisons of experimental with simulation results for a damping scenario with a PDLF controller are shown in Fig. 3. A disturbance is acting on the control signal u, due to the elasticity of the rope. This is more evident when the coupling $-2\frac{\dot{\phi}}{L}\dot{L}$ is small, i.e. $\dot{\phi} \approx 0$. However, the controller performs closely to what is expected from simulations.

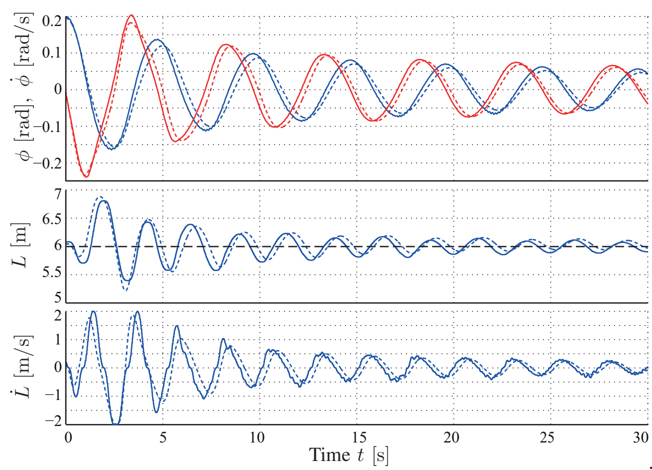

Fig. 3. Validation of PDLF controller in damping scenario. ϕ (blue), $\dot{\phi}$ (red); Simulation (dashed), experiment (solid).

Comparison between CLF and PDLF Approaches: From Figs. 4–6(a) it is apparent that the PDLF approach outperforms the CLF one. The PDLF controller produces a better trade-off between the conflicting objectives, as the damping performance of the PDLF controller is slightly better and the rope length oscillates around its reference. Notice that during hoisting, $\dot{L}$ oscillates about -0.2 [m/s].

Comparison with Previous Approaches: In Fig. 6(b) the PDLF controller is compared with the previous normal form [12] and polytopic LPV [1] controllers. As height increases the LPV controllers outperform the normal form controller, whereas the latter produces a generally more steady control signal.

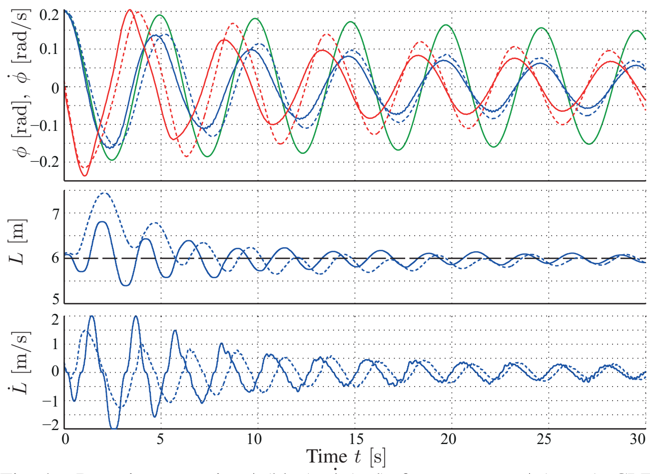

Fig. 4. Damping scenario. ϕ (blue), $\dot{\phi}$ (red), free response ϕ (green); CLF (dashed), PDLF (solid).

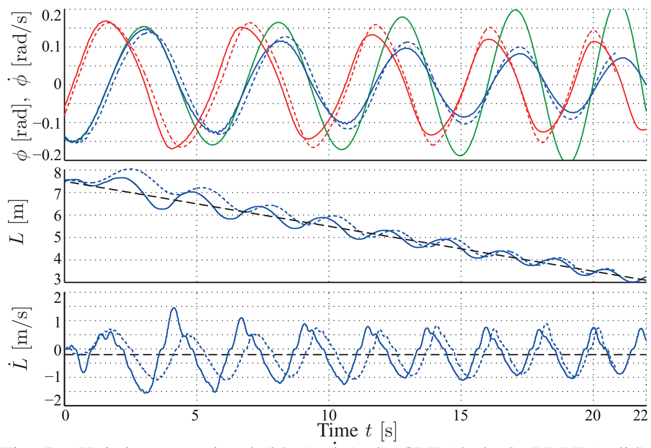

Fig. 5. Hoisting scenario. ϕ (blue), $\dot{\phi}$ (red); CLF (dashed), PDLF (solid); free response (green).

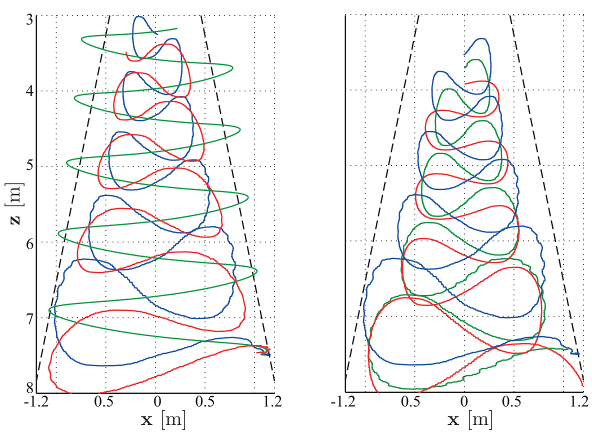

(a) CLF (red), PDLF (blue) and free response (green).

(b) Comparison. Normal form (red), Polytopic LPV (green) and PDLF (blue)

Fig. 6. Hoisting scenario. Container trajectory in cartesian coordinates.

VI. Conclusions

In this paper, a new controller design for the damping of container crane load swing via hoisting modulation has been proposed. The comparison between this approach and previous ones show that some performance is sacrificed for the benefit of taking into account the dynamics of a newly designed observer during synthesis for constant Lyapunov function case. The performance of the previous normal form and polytopic LPV controllers, which have been synthesized neglecting the observer altogether, is recovered by employing parameter-dependent Lyapunov functions. The performance and stability properties offered by the controllers are checked and thus guaranteed by a posteriori analysis of the closed-loop system, which ensures that the system will remain stable with specified performance when it is scheduled with inexact parameters.

References

[1] C. Hoffmann, C. Radisch, and H. Werner, "Active damping of container crane load swing by hoisting modulation - an LPV approach," in *Proceedings of the 51st IEEE Conference on Decision and Control*, 2012, available at www.tuhh.de/~rtsch/HoRaWeCDC2012.

[2] C. Rapp and E. Kreuzer, "Observer design and control of an underactuated crane system," *Proceedings of 2nd Workshop of Research Training Group Ports for Containerships of Future Generations*, vol. 22, pp. 229–241, 2010.

[3] P. Apkarian, P. Gahinet, and G. Becker, "Self-scheduled H_∞ control of linear parameter-varying systems: a design example," *Automatica*, vol. 31, no. 9, pp. 1251–1261, 1995.

[4] A. Kwiatkowski and H. Werner, "PCA-based parameter set mappings for LPV models with fewer parameters and less overbounding," *IEEE Transactions on Control System Technology*, vol. 16, no. 4, pp. 781–788, 2008.

[5] C. Scherer, "LPV control and full block multipliers," *Automatica*, vol. 27, no. 3, pp. 325–485, 2001.

[6] F. Wu and K. Dong, "Gain-scheduling control of LFT systems using parameter-dependent Lyapunov funtions," *Automatica*, vol. 42, no. 1, pp. 39–50, 2006.

[7] S. M. Hashemi and H. Werner, "Gain-scheduled controller synthesis for a nonlinear PDE," *International Journal of Control*, vol. 85, no. 1, pp. 88–97, 2012.

[8] M. Sato, "Gain-scheduled output-feedback controllers using inexactly measured scheduling parameters," in *49th IEEE Conference on Decision and Control*. IEEE, 2010.

[9] ——, "Discrete-time gain-scheduled output-feedback controllers exploiting inexact scheduling parameters via parameter-dependent lyapunov functions," in *50th IEEE Conference on Decision and Control and European Control Conference*. IEEE, 2011.

[10] C. Hoffmann, S. M. Hashemi, H. S. Abbas, and H. Werner, "Closed-loop stability and performance in LPV control based on a reduced parameter set," in *Proceedings of the 51st IEEE Conference on Decision and Control*, 2012, available at www.tuhh.de/~rtsch/HoHaAbWe12.

[11] F. Wu, X. Yang, A. Packard, and G. Becker, "Induced $\mathcal{L}_2$-norm control for LPV systems with bounded parameter variation rates," *International Journal of Nonlinear and Robust Control*, vol. 6, no. 9-10, pp. 983–998, 1996.

[12] C. Rapp, E. Kreuzer, and S. N. Namachchivaya, "Reduced normal form approach to swing control of crane systems: Theory and experiments," *Archive of Applied Mechanics*, 2011.

[13] J. Theis, "Beobachterentwurf für einen räumlich pendelnden körper mit steuerbarer aufhängung," Bachelor Thesis, TUHH, Institut für Mechanik und Meerestechnik, 2010, in German.

[14] S. Ibrir, "LPV approach to continuous and discrete nonlinear observer design," in *28th Chinese Control Conference held jointly with the Conference on Decision and Control*, 2009, pp. 8206–8211.

[15] F. Wu, X. Yang, A. Packard, and G. Becker, "Induced L_2-norm control for LPV system with bounded parameter variation rates," in *Proc. the American Control Conference*, Seatle, Washington, USA, 1995, pp. 2379–2383.

[16] J. F. Sturm, "Using SeDuMi 1.02, a MATLAB toolbox for optimization over symmetric cones," *Optimization Methods and Software*, vol. 11-12, pp. 625–653, 1999.

[17] J. Löfberg, "YALMIP : A toolbox for modeling and optimization in MATLAB," in *Proceedings of the CACSD Conference*, 2004.

[18] P. Apkarian and R. Adams, "Advanced gain-scheduling techniques for uncertain systems," *IEEE Transactions Automatic Control*, vol. 6, no. 1, pp. 21–32, 1998.